The long-term trend and production sensitivity change of the U.S. ozone pollution from observations and model simulations

Hao He[1,2], Xin-Zhong Liang[1,2], Chao Sun[1], Zhining Tao[3,4], and Daniel Q. Tong[1,5]

[1]Department of Atmospheric and Oceanic Science, University of Maryland, College Park, Maryland 20742, USA

[2]Earth System Science Interdisciplinary Center, University of Maryland, College Park, Maryland 20740, USA

[3]Universities Space Research Association, Columbia, Maryland 21046, USA

[4]NASA Goddard Space Flight Center, Greenbelt, Maryland 20771, USA

[5]Center for Spatial Information Science and Systems, George Mason University, Fairfax, VA 22030, USA

Keywords: Air Quality Trend, CMAQ Simulations, Ozone Production Sensitivity

Corresponding to Dr. Xin-Zhong Liang (xliang@umd.edu)

Abstract

We investigated the ozone pollution trend and its sensitivity to key precursors from 1990 to 2015 in the United States using long-term EPA AQS observations and mesoscale simulations. The modeling system, a coupled regional climate – air quality (CWRF-CMAQ) model, well captured summer surface ozone pollution during the past decades, having a mean slope of linear regression with AQS observations at ~0.75. While the AQS network has limited spatial coverage and measures only a few key chemical species, the CWRF-CMAQ provides comprehensive simulations to enable a more rigorous study of the change in ozone pollution and chemical sensitivity. Analysis of seasonal variations and diurnal cycle of ozone observations showed that peak ozone concentrations in the summer afternoon decreased ubiquitously across the United States, up to 0.5 ppbv/yr in major non-attainment areas such as Los Angeles, while concentrations at other hours such as the early morning and late afternoon increased slightly. Consistent with the AQS observations, CMAQ simulated a similar decreasing trend of peak ozone concentrations in the afternoon, up to 0.4 ppbv/yr, and increasing ozone trends in the early morning and late afternoon. A monotonic decreasing trend (up to 0.5 ppbv/yr) in the odd oxygen ($O_x = O_3 + NO_2$) concentrations are simulated by CMAQ at all daytime hours. This result suggests that the increased ozone in the early morning and late afternoon was likely caused by reduced NO-O_3 titration driven by continuous anthropogenic NO_x emission reductions in the past decades. Furthermore, the CMAQ simulations revealed a shift in chemical regimes of ozone photochemical production. From 1990 to 2015, surface ozone production in some metropolitan areas, such as Baltimore, has transited from VOC-sensitive environment (>50% probability) to NO_x-sensitive regime. Our results demonstrated that the long-term CWRF-CMAQ simulations can provide detailed information of the ozone chemistry evolution under a changing climate, and

may partially explain the U.S. ozone pollution responses to regional and national regulations.

1. Introduction

Tropospheric ozone (O_3) is one of the major air pollutants, regulated by the U.S. Environmental Protection Agency (EPA), that pose myriad threats to public health and the environment (Adams et al., 1989; WHO, 2003; Ashmore, 2005; Anderson, 2009; Jerrett et al., 2009). It is also an important greenhouse gas due to the absorption of thermal radiation, affecting the climate (Fishman et al., 1979; Ramanathan and Dickinson, 1979; IPCC, 2013). The major source of tropospheric ozone is photochemical production from ozone precursors such as carbon monoxide (CO), volatile organic compounds (VOCs), and nitrogen oxides (NO_x) at the presence of sunlight (Crutzen, 1974; Seinfeld, 1991; Jacob, 2000; EPA, 2006), while downward transport of stratospheric air mass contributes substantially to ozone concentrations in upper troposphere (Levy et al., 1985; Holton et al., 1995; Stevenson et al., 2006). In the past decades, ozone pollution in the United States has been reduced substantially due to regulations on anthropogenic emissions of ozone precursors (Oltmans et al., 2006; Lefohn et al., 2008, 2010; Cooper et al., 2012; He et al., 2013; Cooper et al., 2014), although some studies suggested no trend or slight increases at some rural areas (Jaffe and Ray, 2007; Lefohn et al., 2010; Cooper et al., 2012). Most of these analyses focused on peak ozone concentrations, e.g., daily maximum 8-hour average ozone (MDA8), during summer, but studies on trends in seasonal and diurnal patterns of ozone pollution are limited. He et al. (2019) analyzed measurements from four monitoring sites in the eastern United States and found different ozone trends between rural and urban sites from the late 1990s to the early 2010s including some increases at certain hours, suggesting effects of national regulations could be regionally dependent. Thus, it is important to extend our study to

64 other regions of the United States in a longer time period.

65 The non-monotonic trends in United States ozone pollution could be caused by the
66 complex non-linear chemistry of ozone production involving NO_x and VOCs (Logan et al., 1981;
67 Finlayson-Pitts and Pitts, 1999; Seinfeld and Pandis, 2006). With continuous reduction of
68 anthropogenic emissions of ozone precursors mainly NO_x and VOCs in the United States, we
69 need to better understand the photochemical regime change for local ozone production (i.e.,
70 ozone production sensitivity), because air pollution regulations could have different effects under
71 NO_x-sensitive and VOC-sensitive environment (Dodge, 1987; Kleinman, 1994). For instance,
72 under a VOC-sensitive photochemical regime, the decrease of NO_x emissions has limited
73 impacts on improving ozone pollution. Previous studies have developed photochemical
74 indicators to identify the ozone production sensitivity (Sillman, 1995; Sillman et al., 1997;
75 Tonnesen and Dennis, 2000b, 2000a; Sillman and He, 2002). Sillman (1999) found the ratio of
76 VOCs and NO_x (VOC/NO_x) has a typical value less than 4 for the VOC-sensitive environment
77 and higher than 15 for the NO_x-sensitive regime. Observation-based studies of ozone production
78 sensitivity relied on research grade measurements of ozone precursors and photochemical
79 intermediates that are not routinely measured by air quality management agencies such as the
80 U.S. EPA. These species include reactive nitrogen compounds (NO_y), nitric acid (HNO_3), and
81 hydrogen peroxide (H_2O_2), normally observed during field campaigns (e.g., Shon et al., 2007;
82 Peng et al., 2011) which only covered limited areas in certain periods. Studies based on air
83 quality models (AQM) could identify the ozone production regimes at regional scales (Sillman et
84 al., 1997; Sillman and He, 2002; Zhang et al., 2009a; Zhang et al., 2009b; Xie et al., 2011), but
85 the simulation periods were usually short (less than one year) and thus could not capture the
86 long-term change in ozone production sensitivity.

Regional AQMs are widely used for investigating the U.S. air quality (Tagaris et al., 2007; Tang et al., 2009; Hogrefe et al., 2011; Pour-Biazar et al., 2011; He et al., 2016a; He et al., 2018). They incorporate finer resolutions, more detailed emissions, and more explicit chemical mechanism than global chemical transport models to better resolve characteristics of tropospheric and surface dynamics, physical and chemical processes essential for air quality. Our group has developed and used coupled regional climate-air quality models to study air quality variations under a changing regional climate (Huang et al., 2007; Zhu and Liang, 2013; He et al., 2016a; He et al., 2018). Our previous studies showed the model's ability to capture the decadal U.S. air quality change (e.g., Zhu and Liang, 2013). In this study, we coupled the latest Climate-Weather Research Forecast (CWRF) and the EPA Community Multiscale Air Quality (CMAQ) models. CWRF has demonstrated substantial improvement in downscaling regional climate and extremes (Liang et al., 2012; Chen et al., 2016; Liu et al., 2016; Liang et al., 2019; Sun and Liang, 2020a; Sun and Liang, 2020b) and thus can provide more realistic weather conditions for AQMs to produce more credible air quality simulations.

To supplement the limited observations in both spatial coverage and chemical species, we conducted a continuous 26-yr CWRF-CMAQ simulation from 1990 to 2015 for a more rigorous analysis of long-term U.S. ozone trend. The model performance of the U.S. air quality was first evaluated against gridded ozone observations. The ozone seasonal variations and diurnal cycles were then extracted to determine the observed long-term trend. The model simulations were subsequently analyzed to explain the observed ozone trends and change in ozone production sensitivity.

2. Observations and model simulations

2.1 Long-term EPA observations

Hourly measurements of surface ozone concentrations from 1990 to 2015 were available from the EPA Air Quality System (AQS) database (https://www.epa.gov/outdoor-air-quality-data). They have been examined following the EPA guidance including the quality assurance and quality control. The locations and durations of AQS monitoring sites have changed substantially due to logistics and requirements to cover the regions sensitive to air pollution. Figure 1 shows that more than 2000 sites which reported ozone measurements during the period of 1990 to 2015. To alleviate the impacts from missing data and short durations, we selected 640 sites that had ozone observation records longer than 20 years. Hourly ozone observations were processed following the approach described in He et al. (2019) to create the long-term seasonal and diurnal records for these stations.

2.2 Regional climate modeling

CWRF (Liang et al., 2012) was driven by the European Centre for Medium-Range Weather Forecasts ERA-Interim reanalysis (ERI, Dee et al., 2011) to downscale regional climate variations during 1989-2015 with the first year as the spin-up and not used. We adopted the well-established CWRF North American domain with a 30-km grid spacing (Fig. 1), covering the Contiguous United States (CONUS) and neighboring southern Canada, northern Mexico and adjacent oceans. The CWRF was developed as a climate extension of the WRF model (Skamarock et al., 2008) incorporating numerous improvements in representation of physical processes and integration of external forcings that are crucial to climate scales, including interactions between land-atmosphere-ocean, convection-microphysics and cloud-aerosol-

radiation, and system consistency throughout all process modules (Liang et al., 2012; Qiao and Liang, 2015; Chen et al., 2016; Liu et al., 2016; Qiao and Liang, 2016). CWRF is built with a comprehensive ensemble of many alternate mainstream parameterization schemed for each of key physical processes. . It has been vigorously tested in North America and Asia showing outstanding performance to capture regional climate characteristics (Yuan and Liang, 2011; Chen et al., 2016; Liu et al., 2016; Liang et al., 2019). The CWRF downscaling has been shown to provide realistic meteorological fields and regional climate signals that can be cordially used to drive the CMAQ for long air quality simulations. Major CWRF physics configurations include the semi-empirical cloudiness parameterization of Xu and Randall (1996), the cloud microphysics scheme of Tao et al. (1989), the short wave and long wave radiation scheme of Chou et al. (2001), the ensemble cumulus parameterization (Qiao and Liang, 2015, 2016; Qiao and Liang, 2017), and the planetary boundary layer scheme of Holtslag and Boville (1993). Hourly CWRF outputs were processed using a modified Meteorology-Chemistry Interface Processor (MCIP, version 4.3) for CMAQ simulations.

2.3 Emissions preparation

To prepare anthropogenic emissions, we chose 2014 as the baseline year. This year's emissions were modified from the National Emissions Inventory 2011 (NEI2011). The modifications was based on measurements from the Ozone Monitoring Instrument (OMI) onboard satellite Aura, the ground-based AQS network, and the *in-situ* continuous emissions monitoring in power plants (Tong et al., 2015; Tong et al., 2016). The so modified NEI2011 inventory was processed using the Sparse Matrix Operator Kernel Emissions (SMOKE) version 3.7 (Houyoux et al., 2000). Emissions from on-road, off-road, and area sources were placed at

154 the model layer closest to the surface. Emissions from point sources, e.g., stacks from power
155 plants, were distributed vertically based on stack height and plume rise. The plume rise was
156 estimated based on the method in Briggs (1972). The inventory pollutants were speciated
157 according to the carbon bond chemical mechanism version 5 (CB05) and AERO5 aerosol
158 mechanism. To fill the gap where NEI2011 data were not available, the Emissions Database for
159 Global Atmospheric Research (EDGAR v3, http://edgar.jrc.ec.europa.eu/) at a 1° × 1° resolution
160 developed by the Joint Research Centre of European Commission was adapted. Figure 2 shows
161 an example of 2010-2015 mean NO_x emissions distribution over the modeling domain. Daily
162 mean NO_x emissions have high values in urban areas of cities such as Los Angeles, Chicago, and
163 the northeast corridor from Washington D.C. to Boston.

164 To project emissions from the baseline year into all individual years, we used the scaling
165 factors from Air Pollutant Emissions Trends (APET) data compiled by the U.S. EPA
166 (https://www.epa.gov/air-emissions-inventories/air-pollutant-emissions-trends-data). Emissions
167 of the baseline year are based on EPA NEI2011 inventory which can provide the best available
168 anthropogenic emissions to the CONUS and are currently used in the operational U.S. national
169 air quality forecast. The usage of APET scaling factors can guarantee the domain total emissions
170 are consistent with the U.S. EPA emissions trend, although assuming the same spatial
171 distribution of anthropogenic emissions from year to year may not be realistic. Without a
172 reasonable observation of actual spatiotemporal variations, it is the cost-effective approach as a
173 first-order approximation to simulate long-term U.S. air quality driven by consistent CONUS
174 total anthropogenic emissions that account interannual trends. Figure 3 shows the emission
175 evolution from 1990 to 2015. Since 1990 anthropogenic emissions of NO_x, CO, sulfur dioxide
176 (SO_2), and VOCs had steady decreasing trends, with SO_2 experiencing the largest reduction. On

177 the other hand, anthropogenic $PM_{2.5}$ and NH_3 emissions stayed mostly flat since the early 2000s.

178 The wildfire emissions were based on the Global Fire Emissions Database, Version 4 with
179 small fires (GFEDv4s, Randerson et al., 2017; van der Werf et al., 2017). The 0.25° × 0.25°
180 degree resolution GFEDv4s data were projected onto the modeling domain and speciated into the
181 CB05 and AERO5 species. GFEDv4s had a monthly resolution from 1997 to 2000 and daily
182 resolution from 2000 onward. Figure 4 illustrates the fire emissions evolution during 1990 to
183 2015 relative to 2014. Fire emissions have large interannual variations, with high emissions in
184 1998, 2002, 2013, and 2015, and low emissions in 2001, 2004, and 2014. We developed a
185 method to merge the aforementioned anthropogenic and wildfire emissions into the
186 temporalized, gridded and speciated data ready for CMAQ.

187 The biogenic emissions were calculated on-line within CMAQ based on the Biogenic
188 Emissions Landuse Database, Version 3 (BELD3, https://www.epa.gov/air-emissions-
189 modeling/biogenic-emissions-landuse-database-version-3-beld3). The 1-km resolution BELD3
190 data with spatial distribution of 230 vegetation classes over the North America were processed
191 through the Spatial Allocator developed by the Community Modeling and Analysis System
192 (CMAS) center (https://www.cmascenter.org/sa-tools/) to generate the gridded vegetation
193 distribution over the study domain. Table 1 lists the 5-yr mean variations of daily major ozone
194 precursor (CO, NO_x, and NMVOCs) emissions in the modeling domain and five subdomains.
195 The emission data show regionally dependent reductions. For instance, compared with 2000-
196 2004, the NO_x emissions in 2005-2009 decreased by ~36% averaged in the CONUS, while 38%
197 and 35% reductions existed in states of California and Texas.

198

2.4 Air quality modeling

The EPA CMAQ model version 5.2 (EPA, 2017) was selected to simulate the U.S. air quality variations driven by CWRF meteorological fields (Section 2.2) and constructed emissions (Section 2.3). Major chemical mechanisms include the Carbon Bond 6 revision 3 (CB6r3) gas phase chemical scheme with updated secondary organic aerosol (SOA) and nitrate chemistry (Yarwood et al., 2010) and the latest AERO6 aerosol scheme (EPA, 2017), which improved U.S. air quality simulations over previous chemical mechanisms (Appel et al., 2016). Chemical initial and boundary conditions were obtained from the default concentration profiles built in CMAQ (EPA, 2017). Simulations were conducted continuously for each 5-year segment (e.g., 1990-1994, 1995-1999, etc.) with two-week spin-up in December prior to each starting years to speed up simulation turn around. Hourly concentrations of ozone and its key precursors such as nitric oxide (NO) and nitrogen dioxide (NO_2) were saved for subsequent analyses.

3. Results

3.1 Evaluation of CMAQ performance

Our previous studies showed that the direct comparison of observation data from monitoring sites and CMAQ results in 30-km grid could introduce inconsistency for evaluating the model performance (He et al., 2016a). The direct comparison is usually conducted through sampling the grid of CMAQ where the AQS site is located, while the distribution of AQS monitoring sites is usually uneven with more sites concentrated in populous urban and suburban areas where high ozone levels prevail. Sampling 30-km CMAQ grids over the locations of AQS measurements, i.e. direct comparison of averaged concentrations in the 900 km^2 CMAQ grid and pointwise AQS observations, could introduce important biases. So we applied the EPA Remote

Sensing Information Gateway (RSIG) software (available at https://www.epa.gov/rsig) to map the site observations onto our CMAQ grid. The RISG has the capability to 're-grid' the AQS observations on a selected model grid using the inverse-distance-weighted method to calculate the gridded mean concentrations (https://www.epa.gov/hesc/how-rsig-regrids-data). Figure 5 compares summer (JJA) mean MDA8 ozone in 2014 between gridded AQS observations and CMAQ outputs and shows that the model can well capture the U.S. ozone pollution, except underestimation in urban areas such as the Los Angeles basin.

Table 2 summarized the statistics of CMAQ performance simulating the summer ozone concentrations during 2000 - 2015 in CONUS and subdomains. Linear regression analyses of MDA8 ozone result in a mean slope value of 0.75 for CONUS, i.e., CMAQ slightly underestimates ozone over the United States. In subdomains, CMAQ performance exhibits large interannual variations. For instance, in Texas the linear regression slope and correlation coefficient ranges from 0.58 to 0.97 and 0.55 to 0.86, respectively. With gradual reduction in anthropogenic emissions, the fluctuations of CMAQ performance could be related to climate signals which control the regional ozone pollution. Future work is needed to identify the relationship between these regional climate variations and the U.S. ozone pollution. Generally, this modeling system has substantially improved performance in the Southeast, California and Texas, and moderately improved performance in the Northeast and Midwest as compared with our previous modeling system (He et al., 2016a), which significantly underestimated the U.S. ozone pollution. One reason is that CWRF with more sophisticated representation of physical processes have the capability to better simulate the U.S. climate especially surface temperature and precipitation (Liang et al., 2012; Chen et al., 2016; Liu et al., 2016; Sun and Liang, 2020a; Sun and Liang, 2020b), which are key to accurate air quality simulations. The evaluation of

CMAQ performance demonstrates the capability of CWRF-CMAQ to credibly simulate historical air quality.

3.2 Long-term ozone trend in AQS observations

We applied a box-averaging technique (He et al., 2016b; He et al., 2019) to analyze ozone measurements at the selected AQS monitoring sites (Fig 1). This approach used an hour by month box to calculate the mean 24-hr diurnal cycle of ozone for each month. Then we calculated the climatology mean over 24 hours by 12 months and the respective anomaly for each month at each AQS site. Figure 6 shows samples of long-term mean ozone concentrations and anomalies at four non-attainment cities: Baltimore, Maryland; Los Angeles, California; Denver, Colorado; and New York City (NYC), New York. The hour by month climatology (left column of Fig. 6) shows that the peak ozone concentrations in the afternoon during the ozone season (April to September) have been reduced significantly in these cities. However, ozone concentrations in the morning (8 am to 12 pm, all local time hereafter) and at night (8 pm to 8 am) increased slightly. These results confirm the effectiveness of recent emission controls which were designed to reduce the peak ozone. But the expansion of ozone at moderate levels (40-50 ppbv), which are higher than the natural background of U.S. ozone (Fiore et al., 2002; Fiore et al., 2003; Wang et al., 2009; Lefohn et al., 2014), could cause negative health impacts.

The anomaly (right column of Fig. 6) shows large variabilities of ozone concentrations because the ozone production is significantly impacted by regional climate (e.g., temperature, precipitation) with interannual and decadal variations. Large ozone reduction occurred after 2003 when the EPA NO_x State Implementation (SIP) call was implemented (He et al., 2013). The anomalies at Los Angeles (Fig. 6b) and NYC (Fig. 6d) shows decreases of the peak ozone in the

afternoon of summer and increases in other times and seasons. For Baltimore and Denver, the peak ozone was not monotonically reduced, but increased in some years after 2002. Given the continuous reduction of anthropogenic emissions in the past decades, the increased ozone pollution in these areas could be caused by other factors, which need further investigations in the future.

We used the linear regression analysis to calculate the slope, correlation (R), and p-value of ozone trend at each local hour. Figure 7 shows ozone trends (slope, unit of ppbv/yr) at AQS sites which are statistically significant ($R^2 > 0.5$, and $p < 0.05$) in the early morning (8 am), at noon (12 pm), in the afternoon (4 pm), and in the evening (8 pm). Consistent results with the four cities (Fig. 6) are found ubiquitously. The peak ozone at noon and in the afternoon generally had a decreasing trend in CONUS, up to 0.5 ppbv/yr, confirming the improved air quality due to regulations, while ozone in the early morning and late afternoon increased slightly at most of monitoring sites. However, AQS sites in the Bay area (San Francisco, California) and Denver had stronger positive trends in the day time. The possible explanations include the trans-pacific transport of ozone and its precursors to the U.S. West Coast (Hudman et al., 2004; Huang et al., 2010; Lin et al., 2012b) and stratosphere-troposphere exchange of ozone to high altitude region (Langford et al., 2009; Lin et al., 2012a).

3.3. Ozone trends derived from CMAQ simulations

We applied the same box-averaging technique to hourly surface ozone simulations in CONUS and conducted the linear regression analysis to estimate the ozone trend at each model grid (Fig. 8). Compared with ozone trends derived from AQS observations (Fig. 7), the CMAQ model successfully captured the spatial pattern and magnitude of change in ozone

pollution. For instance, at 4 pm LT, CMAQ simulated up to 0.4 ppbv/yr decrease in surface ozone in the eastern United States and south region of California state. However, CMAQ simulated statistically insignificant trends (white color in Fig. 8c) at 4 pm LT in the Bay area, Los Angeles, and Denver where AQS observations showed increasing trends (Fig. 7c). The discrepancy occurred because our model used the static chemical lateral conditions (LBCs) that did not include the change of trans-Pacific transport of air pollutants, which were known to elevate the background ozone in the West Coast. Also CMAQ does not contain stratospheric chemistry and hence cannot account the contribution of downward transport of stratospheric ozone to the high altitude region.

Consistent with trends derived from AQS observations, CMAQ also simulated increasing ozone trends in the early morning (8 am LT, Fig. 8a) and late afternoon (8 pm LT, Fig 8d), especially in urban regions such as Los Angeles and Chicago. He et al. (2019) found ozone increases from observations at four sites in the eastern United States and a possible cause suggested by the reduced NO-O_3 titration through examining the trend in odd oxygen (O_x = O_3 + NO_2). Due to known interferences from nitrogen compounds such as NO_x and organic nitrates to standard NO_2 measurements employed by EPA (Fehsenfeld et al., 1987; Dunlea et al., 2007; Dickerson et al., 2019), the analysis of O_x required research grade NO_2 analyzer (e.g., photolytic NO_2 conversion) which are not available in current AQS network. Thus, our simulations provide a unique opportunity to expand such study to the whole CONUS.

Trends in O_x concentrations simulated by CMAQ at 8 am, 12 pm, 4 pm, and 8 pm show a consistent decreasing trend over the modeling domain, up to 0.5 ppbv/yr reductions in the eastern United States (Fig. 9). The result confirms our hypothesis that the reduced NO-O_3 titration elevated surface ozone concentrations in the early morning and late afternoon when the

photochemical production of ozone is low or not active. Nowadays, the EPA ozone standard focuses on peak ozone concentrations, i.e., MDA8 ozone which usually has maximum values at noon or in the early afternoon, so the damage from additional ozone exposure from these elevated ozone concentrations in the early morning and late afternoon is not considered under the current environment policy. These increased ozone levels could offset the benefit from reduced peak ozone in past decades, which needs further investigations to provide scientific evidence for future policy decision.

3.4 Change in photochemical regime

With the continuous reduction of ozone precursor emissions, changes in the complex O_3-NO_x-VOC chemistry are anticipated. We used the O_3/NO_y ratio as the indicator to study the photochemical regime change in the U.S. surface ozone production. The usage of O_3/NO_y ratio was first proposed by Sillman (Sillman, 1995; Sillman et al., 1997). Sillman et al. (Sillman et al., 1997) conducted a case study of observations in urban areas (Atlanta, New York, and Los Angeles) and modeling results from the Urban Airshed Model and suggested the threshold of 7 as the transition region from VOC-sensitive environment to NO_x-sensitive environment. Zhang et al. (2009a; 2009b) expanded this method to the CONUS with 1-year observations and CMAQ simulations (36-km spatial resolution) and suggested a threshold of 15 for ozone pollution at the national scale. In this study, we did not have access to the long-term research grade NO_y observations from the AQS network and did not conduct sensitivity experiments (due to computational resource limit) with reduced NO_x emissions following Sillman et al. (1997), so we have to reply on the O_3/NO_y threshold from literature. We conducted a simple evaluation of our CMAQ results and found the threshold of 7 could be more proper for urban areas and the

337 threshold of 15 should be more applicable for our study of the whole United State (Figure S1 in
338 the supplementary material). Please note that the O_3/NO_y ratio could depend on the modeling
339 framework, so due to the similarity of our modeling system (30-km CMAQ) and the model used
340 in Zhang et al. (2009a; 2009b), our analysis suggest the similar threshold of 15.

341 The threshold of 15 proposed by Zhang et al. (2009b) was adopted to identify the VOC-
342 sensitive or NO_x-sensitive regime, i.e., $O_3/NO_y < 15$ indicating the VOC-sensitive regime. For
343 each local hour, we calculated the probability when O_3/NO_y is lower than 15 in every month.
344 Figure 10 shows the probability of VOC-sensitive regime at 2 pm in July of 1995, 2005, and
345 2015. Most regions dominated by the VOC-sensitive chemistry are urban or suburban where
346 anthropogenic NO_x emissions are relatively high as compared with anthropogenic and/or
347 biogenic VOCs emissions, such as the Los Angeles basin, the Northeast corridor (Washington
348 D.C.-Baltimore-Philadelphia-NYC), and the Chicago metropolitan area. Noting that these maps
349 are created based on ozone photochemical production simulated at the surface level, so the
350 distributions are slightly different from recent studies using satellite data (Duncan et al., 2010;
351 Jin et al., 2017; Ring et al., 2018).

352 We calculated the mean probability of VOC-sensitivity (2 pm in July) in a 3 × 3 CMAQ
353 grid in metropolitan areas of Baltimore, Los Angeles, and NYC from 1990 to 2015 (Fig. 11).
354 CMAQ simulations suggest the transition from VOC-sensitive regime to NO_x-sensitive regime in
355 these urban areas. There were interannual variabilities in the probability of VOC-sensitive
356 photochemistry in Baltimore (~50%) and NYC (~80%) in the 1990s and the early 2000s. After
357 the EPA 2003 NO_x SIP call, anthropogenic NO_x emissions decreased substantially leading to
358 reduced ozone pollution in the eastern United States (He et al., 2013), so the photochemical
359 production of surface ozone is expected to gradually become NO_x-sensitive. In 2015, ozone

photochemical production in Baltimore was dominated by NO_x emissions (only ~20% probability of VOC-sensitive), while NYC had higher probability (>50%) of VOC-sensitive chemistry. In Los Angeles, ozone chemistry slowly leaned to NO_x-sensitive, but until 2015 the local ozone production was still controlled by VOCs emissions. In regions with VOC-sensitive photochemistry in summer, reduction in NO_x emissions had a limited impact on the local rate of ozone production until the photochemistry of ozone production became NO_x-sensitive. Our analysis can partially explain the different responses of ozone pollution in major U.S. cities to national air quality regulations during the past decades (Cooper et al., 2012) and can provide some insights for future policy decision.

4. Conclusions and Discussion

EPA AQS observations in the United States from 1990 to 2015 were analyzed to study the trend in surface ozone seasonal variations and diurnal cycles. We found that the peak ozone concentrations in the afternoon decreased significantly, especially in major non-attainment regions, but the concentrations in the early morning and late afternoon increased slightly. Regional climate-air quality model captured the long-term records of U.S. ozone pollution and suggested that the increased ozone was caused by reduced NO-O_3 titration due to the continuous reduction of NO_x emissions. Model simulations also showed changes in ozone photochemical regime. The U.S. urban/suburban areas generally transited from the VOC-sensitive regime in the early 1990s to more NO_x-sensitive regime recently. But ozone production in some cities such as NYC and Los Angeles are still substantially impacted by VOC emissions. The current national and regional regulations focus on the MDA8 ozone concentrations mainly determined by the peak ozone in the afternoon. Our study revealed the elevated ozone concentrations in the early

morning and late afternoon which must be considered for their impacts on public health. When NO_x emissions are currently the main target of national and regional control measures, our study suggested that regulations on anthropogenic VOCs emissions could be important in certain regions. This study can improve our understanding about the effectiveness of regulations in the past decades and will provide scientific evidence for future policy decision.

Ozone production is highly non-linear, so accurate emissions are essential to simulate its long-term variations. Due to limited resources, we scaled the anthropogenic emissions from a baseline year (2014) to the 1990s using factors derived from the national trend data to construct consistent emissions for the CONUS with respect to the EPA data. This scaling cannot accurately reflect the detailed regional-dependent regulations for individual state such as the 2012 Health Air Act in Maryland (He et al., 2016b). Also, because the GFED data were only available after 1997, the contribution of wildfire emissions to ozone pollution was not included in model simulations between 1990 to 1996. Thus, we anticipated some uncertainties in ozone simulations in the early 1990s. Our model also has limitations to reproduce ozone records in high altitude regions such as Denver because of lacking the stratospheric chemistry in CMAQ and missing the effect of stratosphere-troposphere exchange to surface ozone. Lastly, due to limited resources, our experiments used static chemical LBCs for CMAQ, which excluded the long-range transport of air pollutants into the United States. So our current modeling system cannot take the historical changes of air pollution outside the United State into account. That is, the effect of long-range transport of air pollutants through model domain boundaries is presumed to be secondary to the long-term trends over the United States. For some West Coast regions such as the state of California, the trans-Pacific transport had been enhanced in the past decades and could play a more important role in determining the local air quality. With these increased air pollutant

transported into the United States, our study may underestimate the impacts of domestic emission reductions to U.S. ozone pollution, especially in the West Coast and the Southwest. To accurate evaluate the contribution from trans-boundary emission, dynamic LBCs from a global chemical transport model is needed in the future study.

Code and data availability

EPA AQS observation data are available at https://www.epa.gov/outdoor-air-quality-data. The CMAQ is a community model and is freely available at https://www.cmascenter.org/cmaq/. The ECMWF ERI data are distributed by NCAR (at https://rda.ucar.edu/datasets/ds627.0/). The CWRF model source code is available upon request.

Author contribution

H.H., X.L., and Z.T. designed the experiment; H.H. and C.S. developed the CWRF-CMAQ system and performed the CWRF modeling; Z.T. and D.T. prepared the emission data; H.H. conducted the CMAQ simulations; H.H., Z.T., and C.S. analyzed the data; H.H. prepared the manuscript with contributions from all co-authors.

Competing interests

The authors declare no conflicts of interest.

Acknowledgments

This work was supported by the U.S. Environmental Protection Agency under Assistance Agreement No. RD-83587601. It has not been formally reviewed by EPA. The views expressed in this document are solely those of the authors and do not necessarily reflect those of the

funding Agency. EPA does not endorse any products or commercial services mentioned in this publication. We thank the support of University of Illinois at Urbana-Champaign (UIUC)/USEPA award 20110150701. We thank the National Center for Supercomputing Applications (NCSA) and the National Center for Atmospheric Research (NCAR) Computation and Information System Laboratory for supercomputing support. We thank Dr. Plessel Todd for the help on the RSIG software (https://www.epa.gov/rsig).

References

Adams, R. M., Glyer, J. D., Johnson, S. L., and McCarl, B. A.: A reassessment of the economic-effects of ozone on United-States agriculture, Japca-the Journal of the Air & Waste Management Association, 39, 960-968, 1989.

Anderson, H. R.: Air pollution and mortality: A history, Atmospheric Environment, 43, 142-152, 10.1016/j.atmosenv.2008.09.026, 2009.

Appel, K. W., Napelenok, S. L., Hogrefe, C., Foley, K. M., Pouliot, G., Murphy, B. N., Luecken, D. J., and Heath, N.: Evaluation of the Community Multiscale Air Quality (CMAQ) Model Version 5.2, 2016 CMAS Conference, Chapel Hill, NC., 2016.

Ashmore, M. R.: Assessing the future global impacts of ozone on vegetation, Plant Cell Environ., 28, 949-964, 10.1111/j.1365-3040.2005.01341.x, 2005.

Briggs, G. A.: Chimney plumes in neutral and stable surroundings∗∗Shwartz and Tulin, Atmospheric Environment6, 19–35 (1971), Atmospheric Environment (1967), 6, 507-510, https://doi.org/10.1016/0004-6981(72)90120-5, 1972.

Chen, L. G., Liang, X. Z., DeWitt, D., Samel, A. N., and Wang, J. X. L.: Simulation of seasonal US precipitation and temperature by the nested CWRF-ECHAM system, Climate Dynamics, 46, 879-896, 10.1007/s00382-015-2619-9, 2016.

Chou, M.-D., Suarez, M. J., Liang, X.-Z., Yan, M. M.-H., and Cote, C.: A thermal infrared radiation parameterization for atmospheric studies, 2001.

Cooper, O., Parrish, D., Ziemke, J., Balashov, N., Cupeiro, M., Galbally, I., Gilge, S., Horowitz, L., Jensen, N., and Lamarque, J.-F.: Global distribution and trends of tropospheric ozone: An observation-based review, Elementa: Science of the Anthropocene, 2, 000029, 2014.

Cooper, O. R., Gao, R. S., Tarasick, D., Leblanc, T., and Sweeney, C.: Long-term ozone trends at rural ozone monitoring sites across the United States, 1990-2010, Journal of Geophysical Research-Atmospheres, 117, D22307, 10.1029/2012jd018261, 2012.

Crutzen, P. J.: Photochemical reactions initiated by and influencing ozone in unpolluted tropospheric air, Tellus, 26, 47-57, 1974.

Dee, D. P., Uppala, S. M., Simmons, A. J., Berrisford, P., Poli, P., Kobayashi, S., Andrae, U., Balmaseda, M. A., Balsamo, G., Bauer, P., Bechtold, P., Beljaars, A. C. M., van de Berg, L., Bidlot, J., Bormann, N., Delsol, C., Dragani, R., Fuentes, M., Geer, A. J., Haimberger, L., Healy, S. B., Hersbach, H., Hólm, E. V., Isaksen, L., Kållberg, P., Köhler, M., Matricardi, M., McNally, A. P., Monge-Sanz, B. M., Morcrette, J. J., Park, B. K., Peubey, C., de Rosnay, P., Tavolato, C., Thépaut, J. N., and Vitart, F.: The ERA-Interim reanalysis: configuration and performance of the data assimilation system, Q. J. R. Meteorol. Soc., 137, 553-597, 10.1002/qj.828, 2011.

Dickerson, R. R., Anderson, D. C., and Ren, X.: On the use of data from commercial NOx analyzers for air pollution studies, Atmospheric Environment, 214, 116873, https://doi.org/10.1016/j.atmosenv.2019.116873, 2019.

Dodge, M.: Chemistry of Oxidant Formation: Implications for Designing Effective Control Strategies U.S. Environmental Protection Agency,Washington, D.C. EPA/600/D-87/114 (NTIS PB87179990), 1987.

Duncan, B. N., Yoshida, Y., Olson, J. R., Sillman, S., Martin, R. V., Lamsal, L., Hu, Y. T., Pickering, K. E., Retscher,

C., Allen, D. J., and Crawford, J. H.: Application of OMI observations to a space-based indicator of NOx and VOC controls on surface ozone formation, Atmospheric Environment, 44, 2213-2223, 10.1016/j.atmosenv.2010.03.010, 2010.
Dunlea, E. J., Herndon, S. C., Nelson, D. D., Volkamer, R. M., San Martini, F., Sheehy, P. M., Zahniser, M. S., Shorter, J. H., Wormhoudt, J. C., Lamb, B. K., Allwine, E. J., Gaffney, J. S., Marley, N. A., Grutter, M., Marquez, C., Blanco, S., Cardenas, B., Retama, A., Villegas, C. R. R., Kolb, C. E., Molina, L. T., and Molina, M. J.: Evaluation of nitrogen dioxide chemiluminescence monitors in a polluted urban environment, Atmospheric Chemistry and Physics, 7, 2691-2704, 2007.
EPA: CMAQ (Version 5.2) Scientific Document, Zenodo. http://doi.org/10.5281/zenodo.1167892, 2017.
EPA, U. S.: Air quality criteria for ozone and related photochemical oxidants, Environ. Prot. Agency, , Research Triangle Park, N.C., 2006.
Fehsenfeld, F. C., Dickerson, R. R., Hubler, G., Luke, W. T., Nunnermacker, L. J., Williams, E. J., Roberts, J. M., Calvert, J. G., Curran, C. M., Delany, A. C., Eubank, C. S., Fahey, D. W., Fried, A., Gandrud, B. W., Langford, A. O., Murphy, P. C., Norton, R. B., Pickering, K. E., and Ridley, B. A.: A ground-based intercomparison of NO, NOx, and NOy measurement techniques, Journal of Geophysical Research-Atmospheres, 92, 14710-14722, 1987.
Finlayson-Pitts, B. J., and Pitts, J. N.: Chemistry of the Upper and Lower Atmosphere, 1st ed., Academic Press, UK, 1999.
Fiore, A., Jacob, D. J., Liu, H., Yantosca, R. M., Fairlie, T. D., and Li, Q.: Variability in surface ozone background over the United States: Implications for air quality policy, Journal of Geophysical Research: Atmospheres, 108, 10.1029/2003jd003855, 2003.
Fiore, A. M., Jacob, D. J., Bey, I., Yantosca, R. M., Field, B. D., Fusco, A. C., and Wilkinson, J. G.: Background ozone over the United States in summer: Origin, trend, and contribution to pollution episodes, Journal of Geophysical Research: Atmospheres, 107, ACH 11-11-ACH 11-25, 10.1029/2001jd000982, 2002.
Fishman, J., Ramanathan, V., Crutzen, P. J., and Liu, S. C.: Tropospheric ozone and climate, Nature, 282, 818-820, 10.1038/282818a0, 1979.
He, H., Stehr, J. W., Hains, J. C., Krask, D. J., Doddridge, B. G., Vinnikov, K. Y., Canty, T. P., Hosley, K. M., Salawitch, R. J., Worden, H. M., and Dickerson, R. R.: Trends in emissions and concentrations of air pollutants in the lower troposphere in the Baltimore/Washington airshed from 1997 to 2011, Atmospheric Chemistry and Physics, 13, 7859-7874, 10.5194/acp-13-7859-2013, 2013.
He, H., Liang, X.-Z., Lei, H., and Wuebbles, D. J.: Future U.S. ozone projections dependence on regional emissions, climate change, long-range transport and differences in modeling design, Atmospheric Environment, 128, 124-133, https://doi.org/10.1016/j.atmosenv.2015.12.064, 2016a.
He, H., Vinnikov, K. Y., Li, C., Krotkov, N. A., Jongeward, A. R., Li, Z. Q., Stehr, J. W., Hains, J. C., and Dickerson, R. R.: Response of SO2 and particulate air pollution to local and regional emission controls: A case study in Maryland, Earth Future, 4, 94-109, 10.1002/2015ef000330, 2016b.
He, H., Liang, X. Z., and Wuebbles, D. J.: Effects of emissions change, climate change and long-range transport on regional modeling of future US particulate matter pollution and speciation, Atmospheric Environment, 179, 166-176, 10.1016/j.atmosenv.2018.02.020, 2018.
He, H., Vinnikov, K. Y., Krotkov, N. A., Edgerton, E. S., Schwab, J. J., and Dickerson, R. R.: Chemical climatology of atmospheric pollutants in the eastern United States: Seasonal/diurnal cycles and contrast under clear/cloudy conditions for remote sensing, Atmospheric Environment, 206, 85-107, https://doi.org/10.1016/j.atmosenv.2019.03.003, 2019.
Hogrefe, C., Hao, W., Zalewsky, E. E., Ku, J. Y., Lynn, B., Rosenzweig, C., Schultz, M. G., Rast, S., Newchurch, M. J., Wang, L., Kinney, P. L., and Sistla, G.: An analysis of long-term regional-scale ozone simulations over the Northeastern United States: variability and trends, Atmospheric Chemistry and Physics, 11, 567-582, 10.5194/acp-11-567-2011, 2011.
Holton, J. R., Haynes, P. H., McIntyre, M. E., Douglass, A. R., Rood, R. B., and Pfister, L.: Stratosphere-troposphere exchange, Reviews of Geophysics, 33, 403-439, 10.1029/95rg02097, 1995.
Holtslag, A. A. M., and Boville, B. A.: Local Versus Nonlocal Boundary-Layer Diffusion in a Global Climate Model, Journal of Climate, 6, 1825-1842, 10.1175/1520-0442(1993)006<1825:lvnbld>2.0.co;2, 1993.
Houyoux, M. R., Vukovich, J. M., Coats Jr., C. J., Wheeler, N. J. M., and Kasibhatla, P. S.: Emission inventory development and processing for the Seasonal Model for Regional Air Quality (SMRAQ) project, Journal of Geophysical Research: Atmospheres, 105, 9079-9090, 10.1029/1999jd900975, 2000.
Huang, H. C., Liang, X. Z., Kunkel, K. E., Caughey, M., and Williams, A.: Seasonal simulation of tropospheric ozone over the midwestern and northeastern United States: An application of a coupled regional climate

and air quality modeling system, J. Appl. Meteorol. Climatol., 46, 945-960, 10.1175/jam2521.1, 2007.
Huang, M., Carmichael, G., Adhikary, B., Spak, S., Kulkarni, S., Cheng, Y., Wei, C., Tang, Y., Parrish, D., and Oltmans, S.: Impacts of transported background ozone on California air quality during the ARCTAS-CARB period–a multi-scale modeling study, Atmospheric Chemistry and Physics, 10, 6947-6968, 2010.
Hudman, R., Jacob, D. J., Cooper, O., Evans, M., Heald, C., Park, R., Fehsenfeld, F., Flocke, F., Holloway, J., and Hübler, G.: Ozone production in transpacific Asian pollution plumes and implications for ozone air quality in California, Journal of Geophysical Research: Atmospheres, 109, 2004.
IPCC: Climate Change 2013: The Physical Science Basis., Contribution of Working Group I to the Fifth Assessment Report (AR5) of the Intergovernmental Panel on Climate Change, 1535 pp., doi:10.1017/CBO9781107415324, 2013.
Jacob, D. J.: Heterogeneous chemistry and tropospheric ozone, Atmospheric Environment, 34, 2131-2159, 10.1016/s1352-2310(99)00462-8, 2000.
Jaffe, D., and Ray, J.: Increase in surface ozone at rural sites in the western US, Atmospheric Environment, 41, 5452-5463, 10.1016/j.atmosenv.2007.02.34, 2007.
Jerrett, M., Burnett, R. T., Pope, C. A., Ito, K., Thurston, G., Krewski, D., Shi, Y., Calle, E., and Thun, M.: Long-Term Ozone Exposure and Mortality, N. Engl. J. Med., 360, 1085-1095, 10.1056/NEJMoa0803894, 2009.
Jin, X., Fiore, A. M., Murray, L. T., Valin, L. C., Lamsal, L. N., Duncan, B., Folkert Boersma, K., De Smedt, I., Abad, G. G., Chance, K., and Tonnesen, G. S.: Evaluating a Space-Based Indicator of Surface Ozone-NOx-VOC Sensitivity Over Midlatitude Source Regions and Application to Decadal Trends, Journal of Geophysical Research: Atmospheres, 122, 10,439-410,461, doi:10.1002/2017JD026720, 2017.
Kleinman, L. I.: Low and high NOx tropospheric photochemistry, Journal of Geophysical Research-Atmospheres, 99, 16831-16838, 10.1029/94jd01028, 1994.
Langford, A., Aikin, K., Eubank, C., and Williams, E.: Stratospheric contribution to high surface ozone in Colorado during springtime, Geophysical Research Letters, 36, 2009.
Lefohn, A. S., Shadwick, D., and Oltmans, S. J.: Characterizing long-term changes in surface ozone levels in the United States (1980-2005), Atmospheric Environment, 42, 8252-8262, 10.1016/j.atmosenv.2008.07.060, 2008.
Lefohn, A. S., Shadwick, D., and Oltmans, S. J.: Characterizing changes in surface ozone levels in metropolitan and rural areas in the United States for 1980-2008 and 1994-2008, Atmospheric Environment, 44, 5199-5210, 10.1016/j.atmosenv.2010.08.049, 2010.
Lefohn, A. S., Emery, C., Shadwick, D., Wernli, H., Jung, J., and Oltmans, S. J.: Estimates of background surface ozone concentrations in the United States based on model-derived source apportionment, Atmospheric Environment, 84, 275-288, https://doi.org/10.1016/j.atmosenv.2013.11.033, 2014.
Levy, H., Mahlman, J. D., Moxim, W. J., and Liu, S. C.: Tropospheric ozone - the role of transport, Journal of Geophysical Research-Atmospheres, 90, 3753-3772, 10.1029/JD090iD02p03753, 1985.
Liang, X.-Z., Xu, M., Yuan, X., Ling, T., Choi, H. I., Zhang, F., Chen, L., Liu, S., Su, S., Qiao, F., He, Y., Wang, J. X. L., Kunkel, K. E., Gao, W., Joseph, E., Morris, V., Yu, T.-W., Dudhia, J., and Michalakes, J.: Regional Climate-Weather Research and Forecasting Model, Bulletin of the American Meteorological Society, 93, 1363-1387, 10.1175/bams-d-11-00180.1, 2012.
Liang, X.-Z., Sun, C., Zheng, X., Dai, Y., Xu, M., Choi, H. I., Ling, T., Qiao, F., Kong, X., Bi, X., Song, L., and Wang, F.: CWRF performance at downscaling China climate characteristics, Climate Dynamics, 52, 2159-2184, 10.1007/s00382-018-4257-5, 2019.
Lin, M., Fiore, A. M., Cooper, O. R., Horowitz, L. W., Langford, A. O., Levy, H., Johnson, B. J., Naik, V., Oltmans, S. J., and Senff, C. J.: Springtime high surface ozone events over the western United States: Quantifying the role of stratospheric intrusions, Journal of Geophysical Research: Atmospheres, 117, 2012a.
Lin, M., Fiore, A. M., Horowitz, L. W., Cooper, O. R., Naik, V., Holloway, J., Johnson, B. J., Middlebrook, A. M., Oltmans, S. J., and Pollack, I. B.: Transport of Asian ozone pollution into surface air over the western United States in spring, Journal of Geophysical Research: Atmospheres, 117, 2012b.
Liu, S., Wang, J. X. L., Liang, X.-Z., and Morris, V.: A hybrid approach to improving the skills of seasonal climate outlook at the regional scale, Climate Dynamics, 46, 483-494, 10.1007/s00382-015-2594-1, 2016.
Logan, J. A., Prather, M. J., Wofsy, S. C., and McElroy, M. B.: Tropospheric chemistry - a global perspective, Journal of Geophysical Research-Oceans and Atmospheres, 86, 7210-7254, 10.1029/JC086iC08p07210, 1981.
Oltmans, S. J., Lefohn, A. S., Harris, J. M., Galbally, I., Scheel, H. E., Bodeker, G., Brunke, E., Claude, H., Tarasick, D., Johnson, B. J., Simmonds, P., Shadwick, D., Anlauf, K., Hayden, K., Schmidlin, F., Fujimoto, T., Akagi, K., Meyer, C., Nichol, S., Davies, J., Redondas, A., and Cuevas, E.: Long-term changes in tropospheric

ozone, Atmospheric Environment, 40, 3156-3173, 10.1016/j.atmosenv.2006.01.029, 2006.
Peng, Y. P., Chen, K. S., Wang, H. K., and Lai, C. H.: In Situ Measurements of Hydrogen Peroxide, Nitric Acid and Reactive Nitrogen to Assess the Ozone Sensitivity in Pingtung County, Taiwan, Aerosol and Air Quality Research, 11, 59-69, 10.4209/aaqr.2010.10.0091, 2011.
Pour-Biazar, A., Khan, M., Wang, L. H., Park, Y. H., Newchurch, M., McNider, R. T., Liu, X., Byun, D. W., and Cameron, R.: Utilization of satellite observation of ozone and aerosols in providing initial and boundary condition for regional air quality studies, Journal of Geophysical Research-Atmospheres, 116, D18309, 10.1029/2010jd015200, 2011.
Qiao, F., and Liang, X.-Z.: Effects of cumulus parameterization closures on simulations of summer precipitation over the continental United States, Climate Dynamics, 49, 225-247, 10.1007/s00382-016-3338-6, 2017.
Qiao, F. X., and Liang, X. Z.: Effects of cumulus parameterizations on predictions of summer flood in the Central United States, Climate Dynamics, 45, 727-744, 10.1007/s00382-014-2301-7, 2015.
Qiao, F. X., and Liang, X. Z.: Effects of cumulus parameterization closures on simulations of summer precipitation over the United States coastal oceans, J. Adv. Model. Earth Syst., 8, 764-785, 10.1002/2015ms000621, 2016.
Ramanathan, V., and Dickinson, R. E.: Role of stratospheric ozone in the zonal and seasonal radiative energy-balance of the Earth-troposphere system, Journal of the Atmospheric Sciences, 36, 1084-1104, 1979.
Randerson, J. T., Van Der Werf, G. R., Giglio, L., Collatz, G. J., and Kasibhatla, P. S.: Global Fire Emissions Database, Version 4.1 (GFEDv4). ORNL Distributed Active Archive Center, 2017.
Ring, A. M., Canty, T. P., Anderson, D. C., Vinciguerra, T. P., He, H., Goldberg, D. L., Ehrman, S. H., Dickerson, R. R., and Salawitch, R. J.: Evaluating commercial marine emissions and their role in air quality policy using observations and the CMAQ model, Atmospheric Environment, 173, 96-107, https://doi.org/10.1016/j.atmosenv.2017.10.037, 2018.
Seinfeld, J. H., and Pandis, S. N.: Atmospheric Chemistry and Physics: From Air Pollution to Climate Change, 2nd ed., John Wiley & Sons, Inc., 2006.
Seinfeld, J. H. e. a.: Rethinking the Ozone Problem in Urban and Regional Air Pollution, National Academics Press, Washingtong, DC, 1991.
Shon, Z.-H., Lee, G., Song, S.-K., Lee, M., Han, J., and Lee, D.: Characteristics of reactive nitrogen compounds and other relevant trace gases in the atmosphere at urban and rural areas of Korea during May–June, 2004, Journal of Atmospheric Chemistry, 58, 203-218, 10.1007/s10874-007-9088-4, 2007.
Sillman, S.: The use of NOy, H2O2, and HNO3 as indicators for ozone-NOx-hydrocarbon sensitivity in urban locations, Journal of Geophysical Research-Atmospheres, 100, 14175-14188, 10.1029/94jd02953, 1995.
Sillman, S., He, D., Cardelino, C., and Imhoff, R. E.: The Use of Photochemical Indicators to Evaluate Ozone-NOx-Hydrocarbon Sensitivity: Case Studies from Atlanta, New York, and Los Angeles, J. Air Waste Manage. Assoc., 47, 1030-1040, 10.1080/10962247.1997.11877500, 1997.
Sillman, S.: The relation between ozone, NOx and hydrocarbons in urban and polluted rural environments, Atmospheric Environment, 33, 1821-1845, 10.1016/s1352-2310(98)00345-8, 1999.
Sillman, S., and He, D.: Some theoretical results concerning O3-NOx-VOC chemistry and NOx-VOC indicators, Journal of Geophysical Research: Atmospheres, 107, ACH 26-21-ACH 26-15, 10.1029/2001jd001123, 2002.
Skamarock, W. C., Klemp, J. B., Dudhia, J., Gill, D. O., Barker, D. M., Duda, M. G., Huang, X.-Y., Wang, W., and Powers, J. G.: A Description of the Advanced Research WRF Version 3, NCAR Technical Note, NCAR/TN-475+STR, 113 pp, 2008.
Stevenson, D. S., Dentener, F. J., Schultz, M. G., Ellingsen, K., van Noije, T. P. C., Wild, O., Zeng, G., Amann, M., Atherton, C. S., Bell, N., Bergmann, D. J., Bey, I., Butler, T., Cofala, J., Collins, W. J., Derwent, R. G., Doherty, R. M., Drevet, J., Eskes, H. J., Fiore, A. M., Gauss, M., Hauglustaine, D. A., Horowitz, L. W., Isaksen, I. S. A., Krol, M. C., Lamarque, J. F., Lawrence, M. G., Montanaro, V., Muller, J. F., Pitari, G., Prather, M. J., Pyle, J. A., Rast, S., Rodriguez, J. M., Sanderson, M. G., Savage, N. H., Shindell, D. T., Strahan, S. E., Sudo, K., and Szopa, S.: Multimodel ensemble simulations of present-day and near-future tropospheric ozone, Journal of Geophysical Research-Atmospheres, 111, D08301, 10.1029/2005jd006338, 2006.
Sun, C., and Liang, X. Z.: Improving U.S. extreme precipitation simulation: Dependence on cumulus parameterization and underlying mechanism, Climate Dynamics, to be submitted, 2020a.
Sun, C., and Liang, X. Z.: Improving U.S. extreme precipitation simulation: Sensitivity to physics parameterizations, Climate Dynamics, to be submitted, 2020b.
Tagaris, E., Manomaiphiboon, K., Liao, K.-J., Leung, L. R., Woo, J.-H., He, S., Amar, P., and Russell, A. G.:

Impacts of global climate change and emissions on regional ozone and fine particulate matter concentrations over the United States, Journal of Geophysical Research: Atmospheres, 112, doi:10.1029/2006JD008262, 2007.

Tang, Y., Lee, P., Tsidulko, M., Huang, H.-C., McQueen, J. T., DiMego, G. J., Emmons, L. K., Pierce, R. B., Thompson, A. M., Lin, H.-M., Kang, D., Tong, D., Yu, S., Mathur, R., Pleim, J. E., Otte, T. L., Pouliot, G., Young, J. O., Schere, K. L., Davidson, P. M., and Stajner, I.: The impact of chemical lateral boundary conditions on CMAQ predictions of tropospheric ozone over the continental United States, Environmental Fluid Mechanics, 9, 43-58, 10.1007/s10652-008-9092-5, 2009.

Tao, W.-K., Simpson, J., and McCumber, M.: An Ice-Water Saturation Adjustment, Mon. Weather Rev., 117, 231-235, 10.1175/1520-0493(1989)117<0231:aiwsa>2.0.co;2, 1989.

Tong, D., Pan, L., Chen, W., Lamsal, L., Lee, P., Tang, Y., Kim, H., Kondragunta, S., and Stajner, I.: Impact of the 2008 Global Recession on air quality over the United States: Implications for surface ozone levels from changes in NOx emissions, Geophysical Research Letters, 43, 9280-9288, 10.1002/2016gl069885, 2016.

Tong, D. Q., Lamsal, L., Pan, L., Ding, C., Kim, H., Lee, P., Chai, T. F., Pickering, K. E., and Stajner, I.: Long-term NOx trends over large cities in the United States during the great recession: Comparison of satellite retrievals, ground observations, and emission inventories, Atmospheric Environment, 107, 70-84, 10.1016/j.atmosenv.2015.01.035, 2015.

Tonnesen, G. S., and Dennis, R. L.: Analysis of radical propagation efficiency to assess ozone sensitivity to hydrocarbons and NO x : 1. Local indicators of instantaneous odd oxygen production sensitivity, Journal of Geophysical Research: Atmospheres, 105, 9213-9225, 10.1029/1999jd900371, 2000a.

Tonnesen, G. S., and Dennis, R. L.: Analysis of radical propagation efficiency to assess ozone sensitivity to hydrocarbons and NO x : 2. Long-lived species as indicators of ozone concentration sensitivity, Journal of Geophysical Research: Atmospheres, 105, 9227-9241, 10.1029/1999jd900372, 2000b.

van der Werf, G. R., Randerson, J. T., Giglio, L., van Leeuwen, T. T., Chen, Y., Rogers, B. M., Mu, M. Q., van Marle, M. J. E., Morton, D. C., Collatz, G. J., Yokelson, R. J., and Kasibhatla, P. S.: Global fire emissions estimates during 1997-2016, Earth Syst. Sci. Data, 9, 697-720, 10.5194/essd-9-697-2017, 2017.

Wang, H., Jacob, D. J., Le Sager, P., Streets, D. G., Park, R. J., Gilliland, A. B., and van Donkelaar, A.: Surface ozone background in the United States: Canadian and Mexican pollution influences, Atmospheric Environment, 43, 1310-1319, https://doi.org/10.1016/j.atmosenv.2008.11.036, 2009.

WHO: Health aspects of air pollution with particulate matter, ozone and nitrogen dioxide, Wolrd Health Organisation, Bonn,, 2003.

Xie, Y., Elleman, R., Jobson, T., and Lamb, B.: Evaluation of O3-NOx-VOC sensitivities predicted with the CMAQ photochemical model using Pacific Northwest 2001 field observations, Journal of Geophysical Research: Atmospheres, 116, 10.1029/2011jd015801, 2011.

Xu, K.-M., and Randall, D. A.: A Semiempirical Cloudiness Parameterization for Use in Climate Models, Journal of the Atmospheric Sciences, 53, 3084-3102, 10.1175/1520-0469(1996)053<3084:ascpfu>2.0.co;2, 1996.

Yarwood, G. S., Whitten, G. Z., Jung, J., Heo, G., and Allen, D.: Development, Evaluation and Testing of Version 6 of the Carbon Bond Chemical Mechanism (CB6), https://www.tceq.texas.gov/assets/public/implementation/air/am/contracts/reports/pm/5820784005FY1026-20100922-environ-cb6.pdf, 2010.

Yuan, X., and Liang, X. Z.: Improving cold season precipitation prediction by the nested CWRF-CFS system, Geophysical Research Letters, 38, L02706, 10.1029/2010gl046104, 2011.

Zhang, Y., Vijayaraghavan, K., Wen, X. Y., Snell, H. E., and Jacobson, M. Z.: Probing into regional ozone and particulate matter pollution in the United States: 1. A 1 year CMAQ simulation and evaluation using surface and satellite data, Journal of Geophysical Research-Atmospheres, 114, 10.1029/2009jd011898, 2009a.

Zhang, Y., Wen, X. Y., Wang, K., Vijayaraghavan, K., and Jacobson, M. Z.: Probing into regional O-3 and particulate matter pollution in the United States: 2. An examination of formation mechanisms through a process analysis technique and sensitivity study, Journal of Geophysical Research-Atmospheres, 114, 10.1029/2009jd011900, 2009b.

Zhu, J. H., and Liang, X. Z.: Impacts of the Bermuda High on Regional Climate and Ozone over the United States, Journal of Climate, 26, 1018-1032, 10.1175/jcli-d-12-00168.1, 2013.

Tables and Figures

Table 1. Summary of multiyear mean average of daily CO, NO_x, and NMVOCs emissions in the CONUS and five subdomains. (Unit: mol/km^2 per second) Please note that our California and Texas subdomains include more area than the states of California and Texas.

CONUS					**Southeast**		
Year	CO	NO_x	NMVOCs		CO	NO_x	NMVOCs
1990-1994	32.9	1.24	0.94		47.2	1.43	1.03
1995-1999	26.2	1.18	0.76		37.4	1.36	0.85
2000-2004	18.9	1.26	0.69		26.4	1.46	0.72
2005-2009	12.3	0.94	0.60		16.9	1.07	0.59
2010-2015	8.0	0.60	0.46		11.0	0.66	0.45
California					**Northeast**		
1990-1994	18.3	1.22	0.57		110.3	3.29	2.12
1995-1999	14.6	1.16	0.46		87.2	3.16	1.68
2000-2004	10.6	1.23	0.40		62.1	3.41	1.43
2005-2009	7.1	0.91	0.35		40.3	2.56	1.25
2010-2015	4.6	0.56	0.26		25.9	1.62	0.93
Texas					**Midwest**		
1990-1994	22.6	1.21	1.26		58.2	1.88	1.41
1995-1999	18.1	1.15	1.03		46.3	1.80	1.14
2000-2004	13.0	1.20	1.01		33.4	1.92	0.98
2005-2009	8.4	0.91	0.92		22.0	1.44	0.85
2010-2015	5.5	0.60	0.73		14.3	0.91	0.63

Table 2. Summary about the comparison of JJA MDA8 ozone concentrations from AQS observations and CMAQ simulations during 2000-2015 in the CONUS and subdomains. Slope and Correlation (Corr. R) are calculated for each year based on linear regression analysis. Please note that our California and Texas subdomains include more area than the states of California and Texas.

Year	Slope	Corr. R	NMB	RMSE	**Year**	Slope	Corr. R	NMB	RMSE
CONUS									
2000	0.73	0.37	-6.9	10.5	**2008**	0.70	0.54	-5.4	8.4
2001	0.80	0.61	-7.7	8.7	**2009**	0.78	0.35	-1.6	8.5
2002	0.71	0.63	-8.6	9.2	**2010**	0.75	0.51	-6.2	8.4
2003	0.81	0.60	-4.3	8.4	**2011**	0.77	0.42	-7.1	9.2
2004	0.85	0.39	1.3	8.9	**2012**	0.67	0.60	-10.7	9.3
2005	0.87	0.54	-7.3	8.8	**2013**	0.70	0.50	-1.8	7.9
2006	0.77	0.48	-7.6	9.1	**2014**	0.72	0.44	-3.0	7.6
2007	0.70	0.60	-6.1	8.0	**2015**	0.73	0.41	-4.2	7.7
California									
2000	0.70	0.67	-19.3	15.2	**2008**	0.63	0.53	-18.0	14.8
2001	0.72	0.63	-18.1	14.8	**2009**	0.67	0.61	-19.0	13.5
2002	0.80	0.55	-15.5	14.4	**2010**	0.62	0.55	-19.0	14.1
2003	0.80	0.55	-20.1	16.2	**2011**	0.68	0.57	-17.0	13.3
2004	0.78	0.51	-19.2	16.1	**2012**	0.64	0.63	-21.4	14.9
2005	0.78	0.54	-19.0	15.3	**2013**	0.64	0.60	-17.9	13.5
2006	0.80	0.61	-20.5	15.6	**2014**	0.69	0.56	-21.9	14.8
2007	0.69	0.65	-16.0	12.9	**2015**	0.72	0.61	-22.3	14.2
Texas									
2000	0.60	0.77	-20.4	11.8	**2008**	0.62	0.74	-10.5	6.6
2001	0.58	0.62	-19.6	11.5	**2009**	0.73	0.78	-17.1	8.7
2002	0.70	0.72	-10.4	6.6	**2010**	0.65	0.77	-9.4	5.3
2003	0.64	0.78	-8.8	6.5	**2011**	0.52	0.83	-22.7	12.1
2004	0.97	0.55	-7.2	5.8	**2012**	0.53	0.86	-17.8	9.4
2005	0.70	0.78	-21.5	11.4	**2013**	0.53	0.74	-11.6	6.9
2006	0.66	0.83	-20.5	11.3	**2014**	0.66	0.72	-5.0	4.7
2007	0.77	0.84	-4.0	3.9	**2015**	0.76	0.61	-10.1	5.8
Southeast									
2000	0.61	0.41	-20.5	13.3	**2008**	0.52	0.77	-13.4	8.3
2001	0.64	0.70	-7.7	6.2	**2009**	0.88	0.52	-2.7	4.2

2002	0.56	0.77	-14.1	9.5	**2010**	0.69	0.75	-7.8	5.1
2003	0.65	0.77	-0.7	4.7	**2011**	0.84	0.62	-13.5	8.2
2004	0.81	0.59	3.2	4.4	**2012**	0.62	0.73	-9.4	6.1
2005	0.54	0.64	-8.8	6	**2013**	0.74	0.70	7.0	4.1
2006	0.74	0.60	-14	9	**2014**	0.84	0.40	0.9	4.0
2007	0.56	0.71	-14.1	9	**2015**	0.71	0.44	-2.6	4.2
Northeast									
2000	0.50	0.25	7.9	7.0	**2008**	0.46	0.11	-0.5	5.8
2001	0.46	0.28	-3.6	6.0	**2009**	0.67	0.23	13.7	7.3
2002	0.51	0.13	-8.5	8.3	**2010**	0.49	0.10	-0.4	5.6
2003	0.85	0.16	3.0	5.3	**2011**	0.47	0.31	3.2	5.9
2004	0.81	0.21	10.0	6.6	**2012**	0.55	0.17	-2.9	5.3
2005	0.84	0.11	2.5	5.8	**2013**	0.78	0.45	11.6	6.4
2006	0.45	0.21	3.0	6.0	**2014**	0.60	0.33	-4.8	5.1
2007	0.48	0.19	-0.7	5.6	**2015**	0.49	0.11	2.2	5.1
Midwest									
2000	0.41	0.25	3.4	5.9	**2008**	0.44	0.25	3.5	4.7
2001	0.55	0.30	-2.3	4.9	**2009**	0.54	0.22	14	7.2
2002	0.45	0.27	-5.2	7.0	**2010**	0.57	0.12	2.4	5.3
2003	0.66	0.25	-0.1	4.7	**2011**	0.45	0.21	1.1	5.6
2004	0.68	0.44	13.9	7.5	**2012**	0.46	0.19	-11.6	8.3
2005	0.76	0.15	-4.4	5.6	**2013**	0.74	0.18	4.9	4.0
2006	0.50	0.17	0.3	5.0	**2014**	0.64	0.20	5.7	4.1
2007	0.39	0.20	-0.6	5.6	**2015**	0.68	0.27	8.7	4.7

711 NMB: Normalized Mean Bias (Unit: %)
712 RMSE: Root Mean Square Error (Unit: ppbv)
713

Figure 1. Locations of EPA AQS sites for surface ozone monitoring during 1990-2015. Red dots stand for monitoring sites with more than 20 year record. Black dots show the locations of monitoring sites have short data records which are not used in this study. The map shows the CWRF-CMAQ 30-km domain and five subdomains sensitive to air pollution. CA: California (including nearby parts of Nevada, Arizona and Oregon); TX: Texas (including nearby parts of Louisiana, Arkansas, and Oklahoma); SE: Southeast; NE: Northeast; MW: Midwest. Please note that our CA and TX subdomains include more area than the states of California and Texas.

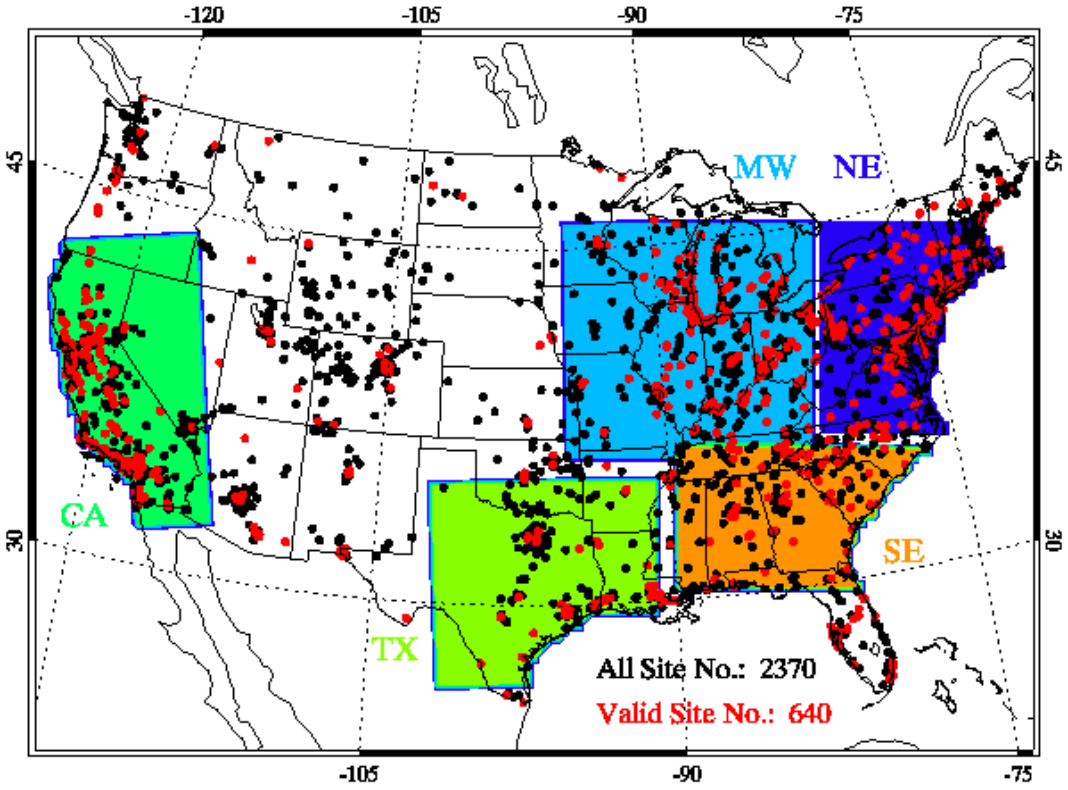

Figure 2. Averaged daily NO_x emissions between 2010 and 2015 in the modeling domain (Unit: mol/km^2 per second).

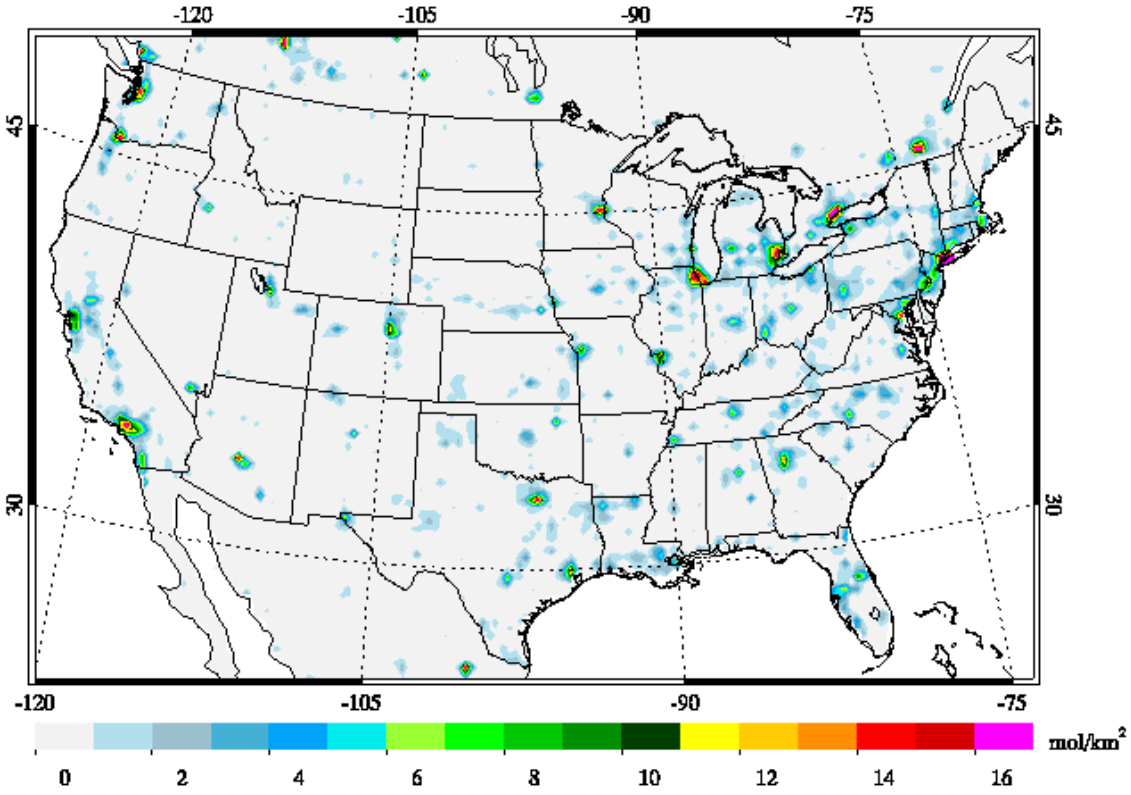

Figure 3. Anthropogenic emission evolution relative to 2014 in the modeling domain from 1990 – 2015.

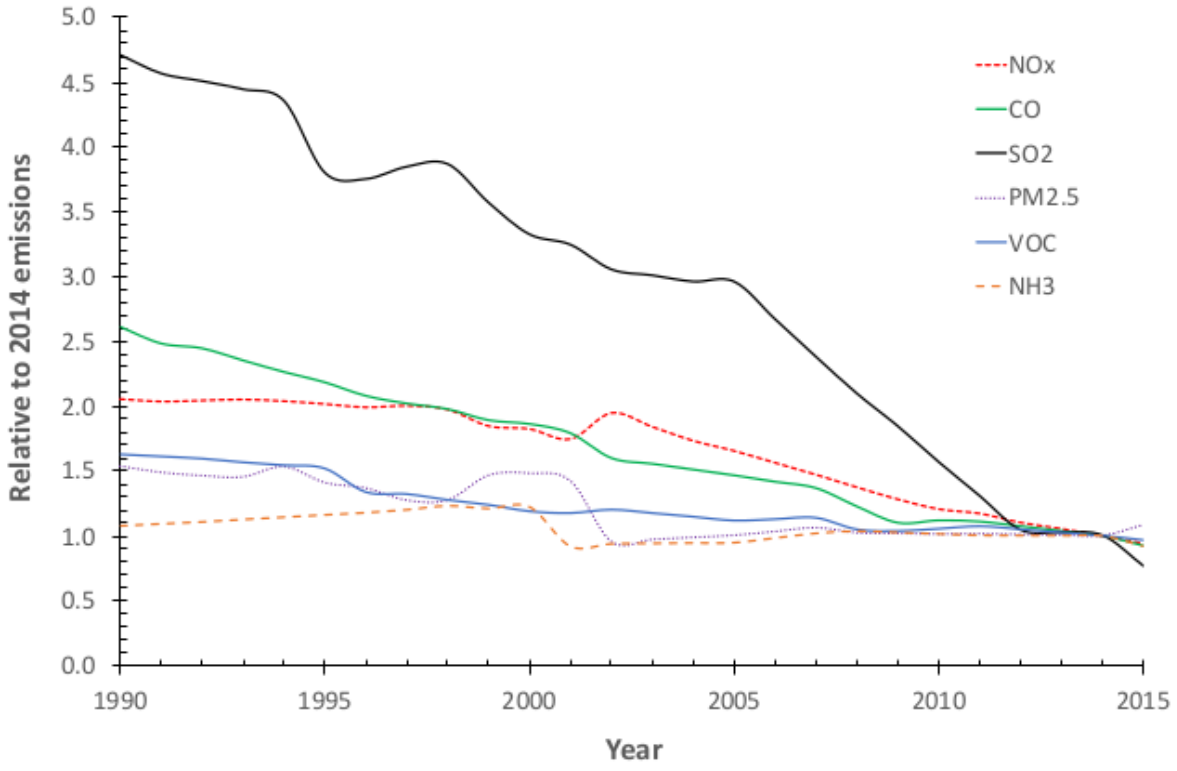

Figure 4. Fire emission evolution relative to 2014 in the modeling domain from 1990 – 2015. Noting that GFED fire emissions are not available before 1997.

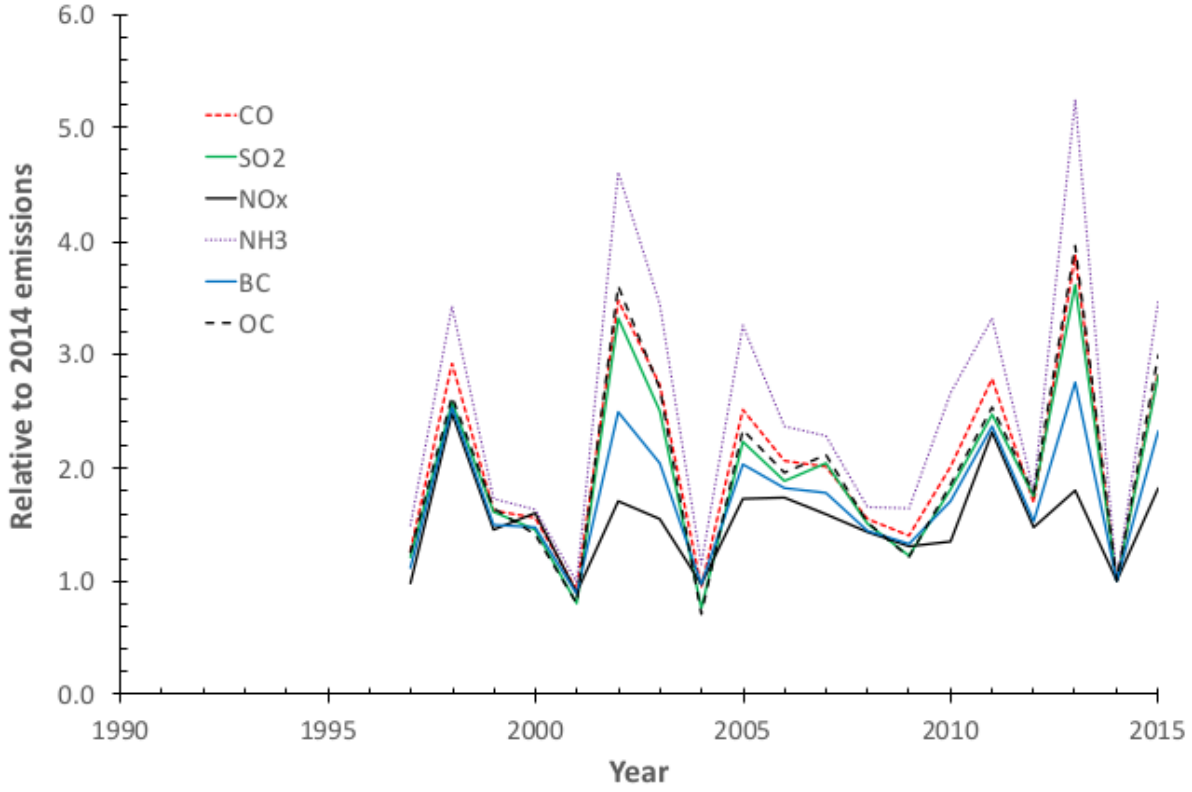

Figure 5. Comparison of summer MDA8 ozone concentrations from EPA AQS observations and CMAQ simulations in 2014. AQS station data were gridded to the CMAQ grid using the EPA RSIG software. a) Contour plot, the background stands for the CMAQ outputs and the dots stand for gridded AQS observations; b) Scatter plot of the gridded AQS observations and co-located CMAQ outputs.

a)

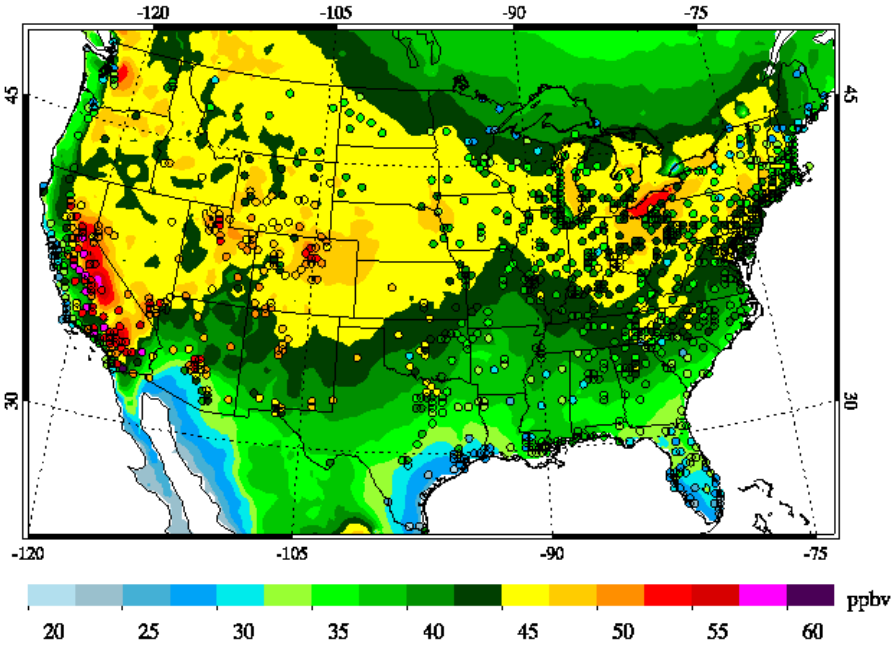

b)

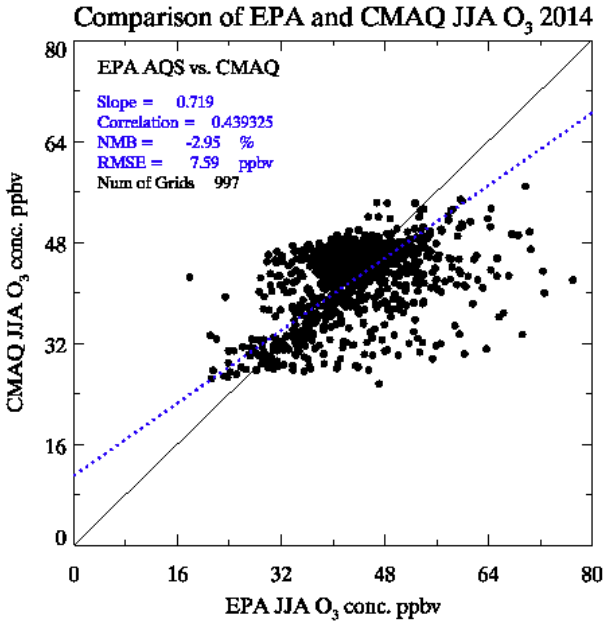

Figure 6. The box-averaging analyses of AQS ozone observations at selected sites from 1990-2015. a) Essex, Maryland (suburban Baltimore, AQS ID 240053001); b) Pasadena, California (downtown Los Angeles, AQS ID 060372005); c) Denver, Colorado (downtown Denver, AQS ID 080310014); d) Staten Island, New York (suburban New York City, AQS ID: 360850067). Left column shows the monthly mean, right column shows the anomaly values. White patches stand for missing data or not sufficient data for the box-averaging analysis.

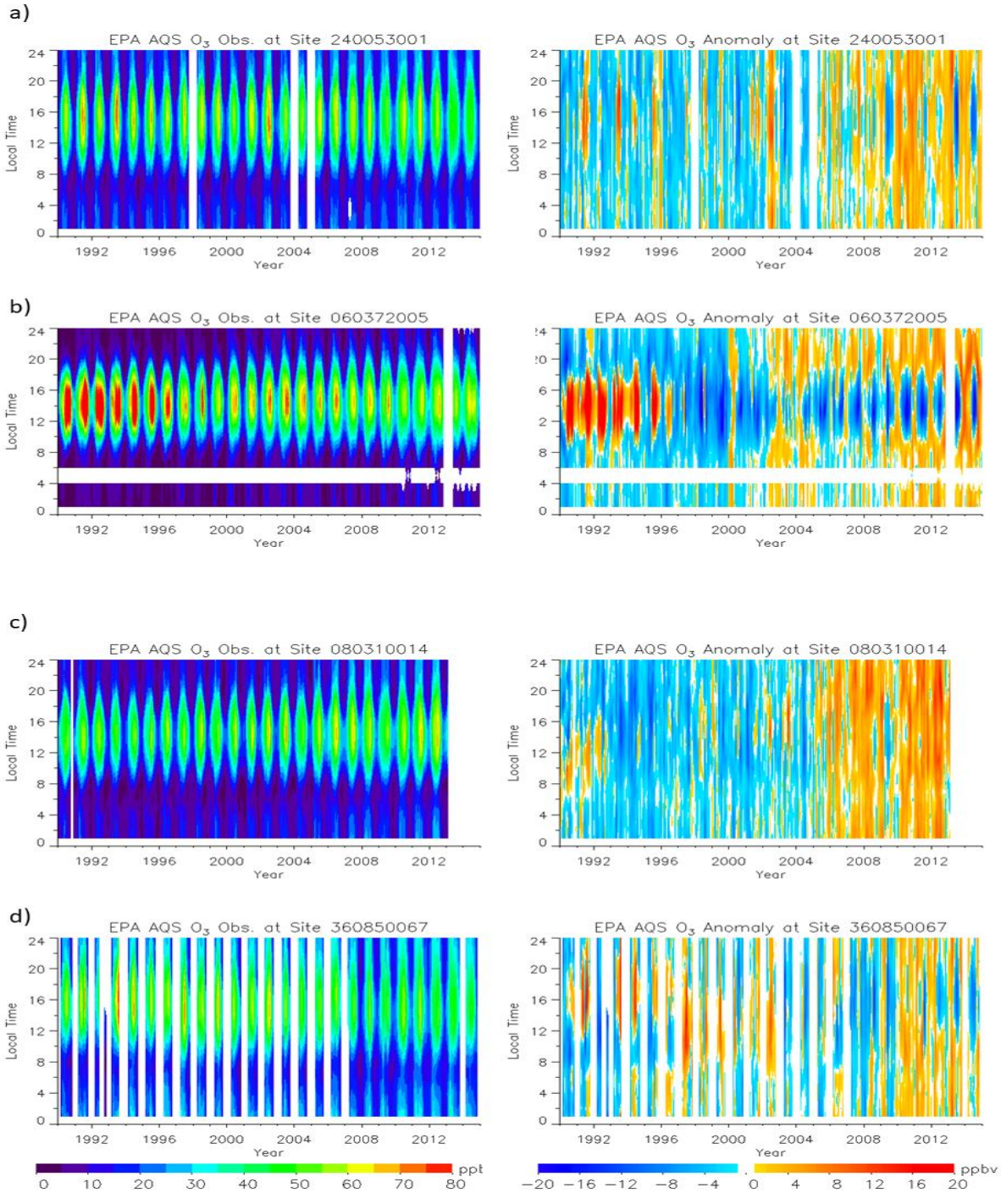

Figure 7. Trend in ozone observations at selected EPA AQS sites during 1990-2015 (Unit: ppbv/yr). a) at 8 am; b) at 12 pm; c) at 4 pm; d) at 8 pm (all local time). We only show the sites with statistically significant linear trend in the plots.

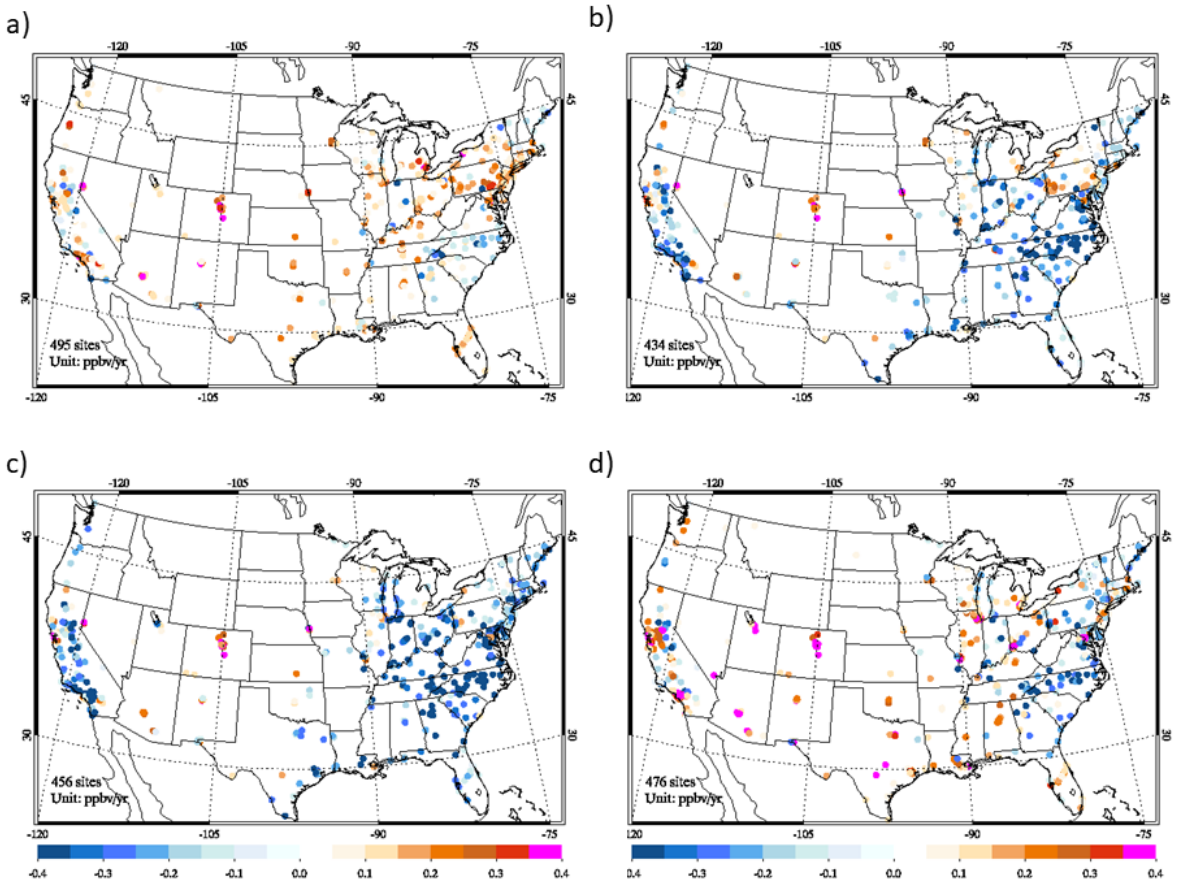

Figure 8. Trends in ozone simulations from CMAQ during 1990-2015 (Unit: ppbv/yr). a) at 8 am; b) at 12 pm; c) at 4 pm; d) at 8 pm (all local time). We only show CMAQ grids with statistically significant linear trend in the plots.

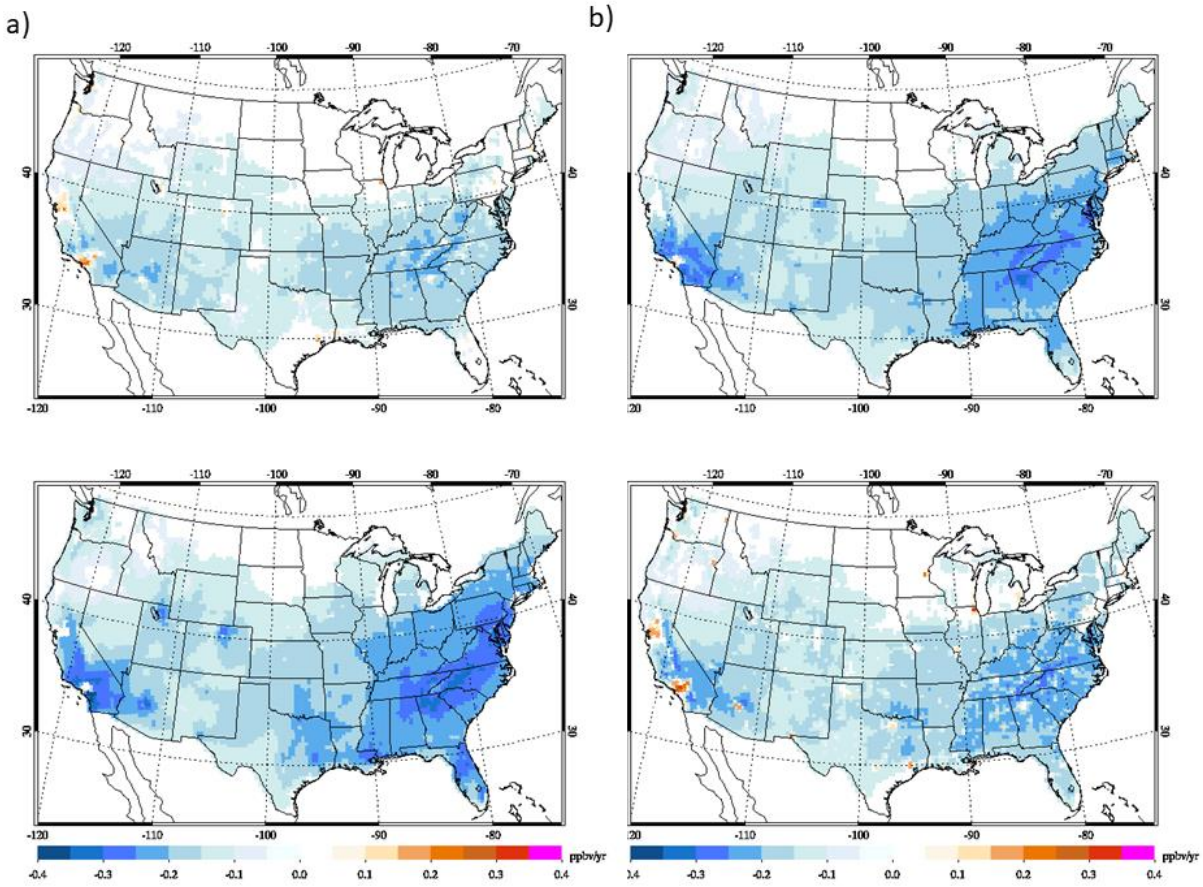

Figure 9. Trend in O_x ($O_x = O_3 + NO_2$) simulated by CMAQ during 1990-2015. a) at 8 am; b) at 12 am; c) at 4 pm; d) at 8 pm (all local time). We only show CMAQ grids with statistically significant linear trend in the plots.

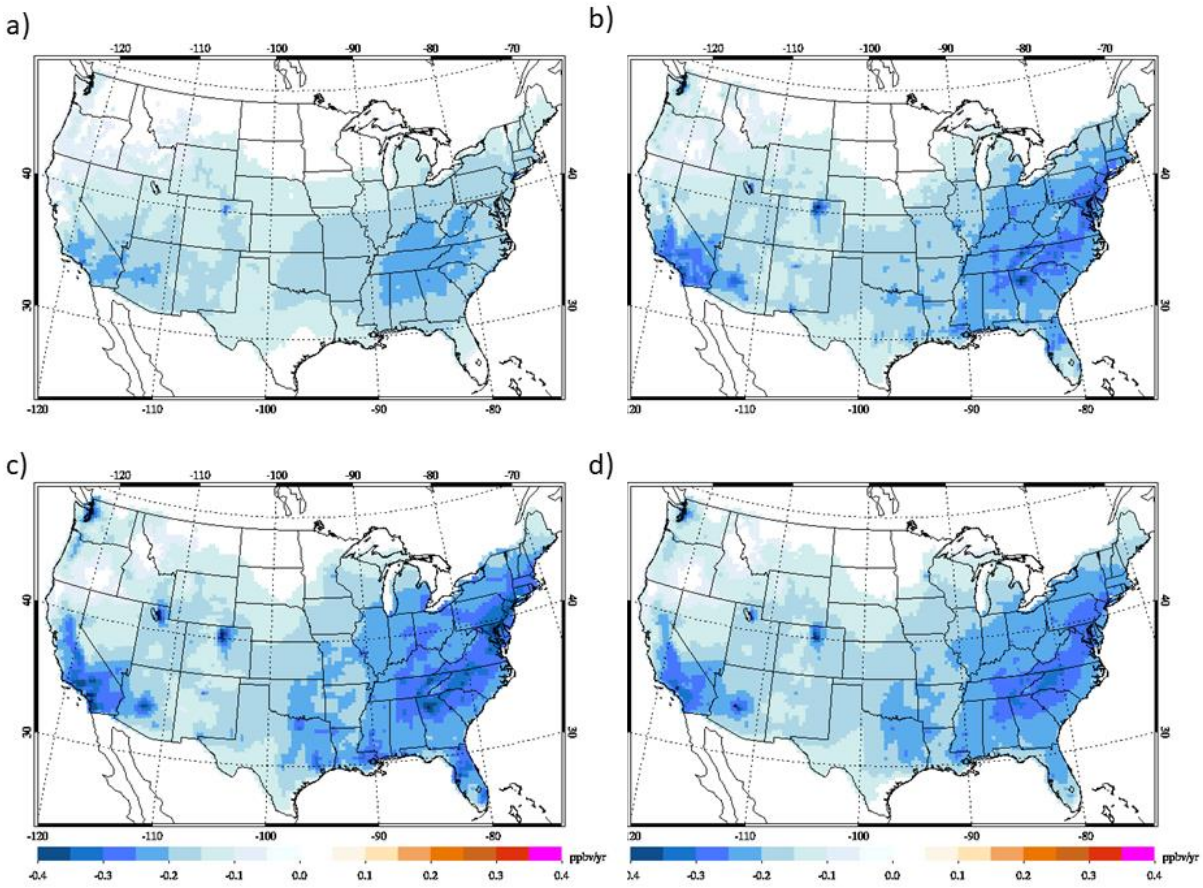

Figure 10. Probability of VOC-sensitive photochemical ozone production (i.e., $O_3/NO_y < 15$) in the CONUS simulated by CMAQ at 2 pm local time in July, a) 1995; b) 2005; and c) 2015

a)

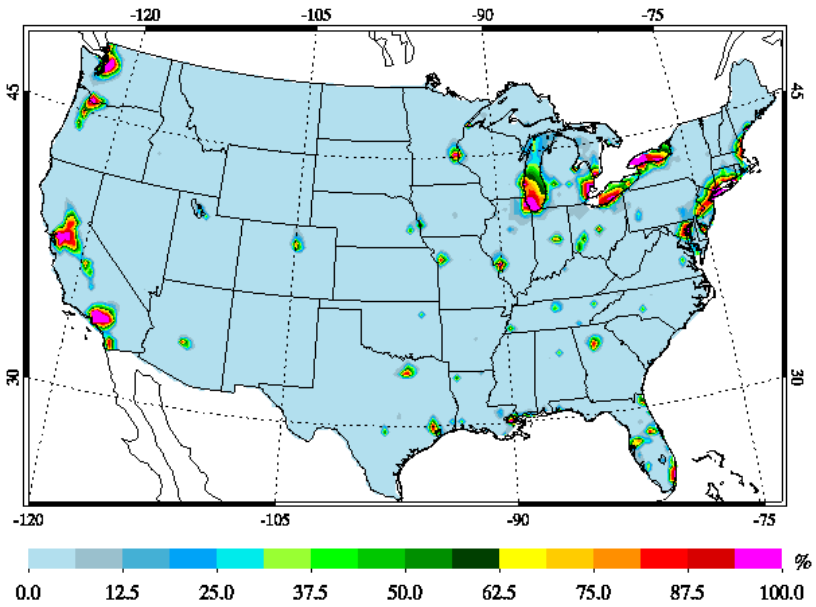

b)

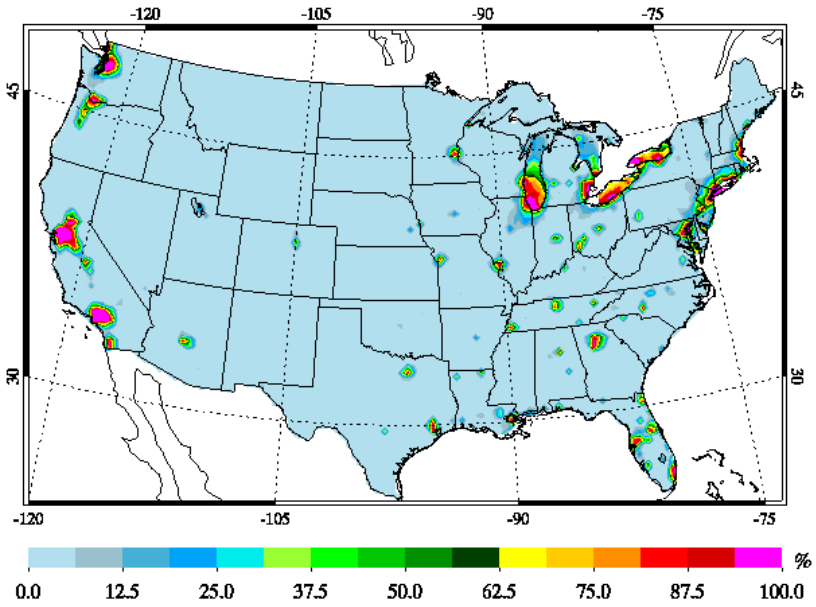

769 c)

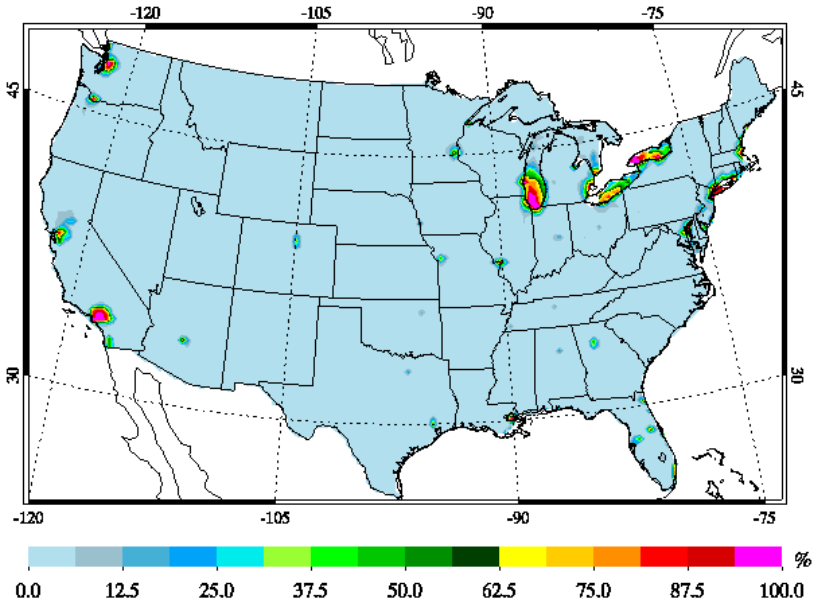

770

771 **Figure 11.** Long-term trends in probability of VOC-sensitive photochemical production of
772 surface ozone in three major urban areas at 2 pm in July. Probability is calculated using averages
773 of 3 × 3 grids centered at downtown.

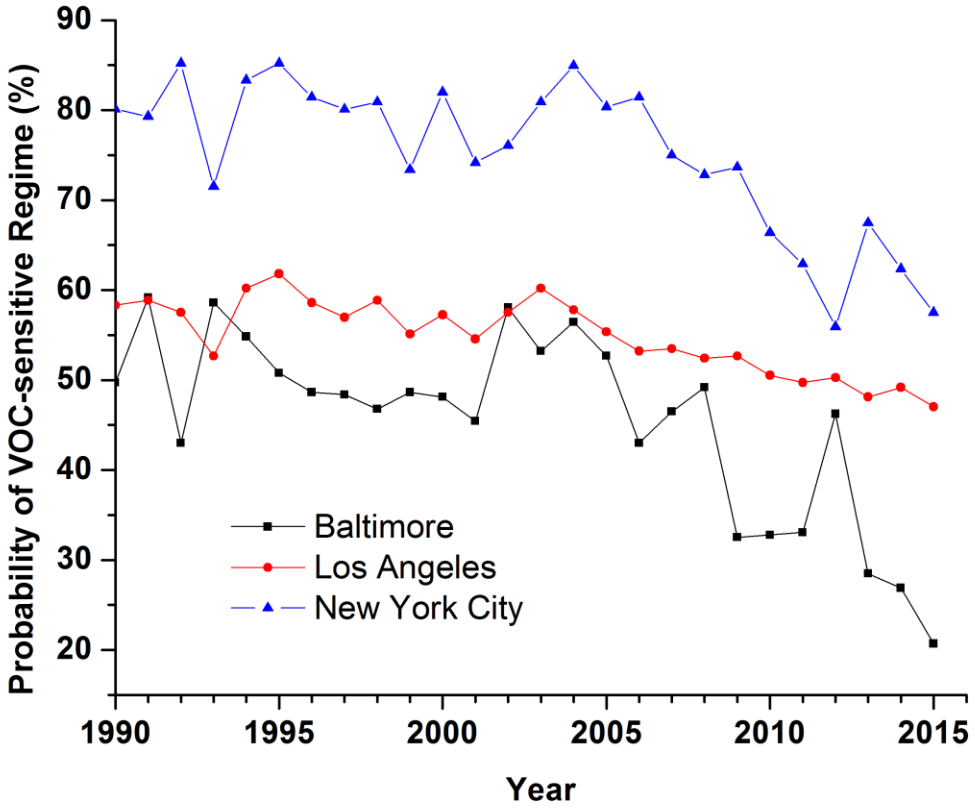

774